regenerates the neutral complex. Dichloromethane solutions of $Ph_4As[Os_2(\mu\text{-}O)(\mu\text{-}O_2CCH_3)_2Cl_4(PPh_3)_2]$ (containing 0.2 M TBAH as supporting electrolyte) exhibit an oxidation at $E_{1/2} = +0.20$ V vs. SCE and an irreversible reduction at $E_{p,c} \simeq -0.97$ V. Acetonitrile solutions of the sodium and tetraphenylarsonium salts (0.1 M in TBAH) have a reversible oxidation at $E_{1/2} = +0.31$ V vs. SCE; the same couple is observed in acetonitrile solutions of the neutral derivative, but it now corresponds to a reduction (see footnote *c* in Table V). Solutions of $Ph_4As[Os_2(\mu\text{-}O)(\mu\text{-}O_2CCH_3)_2Cl_4(PPh_3)_2]$ in dichloromethane have electronic absorption spectra that exhibit an intense absorption at 487 nm (an acetone solution of the sodium salt has this band maximum at 500 nm) and a weaker band at ~1060 nm ($\epsilon \sim 500$). The latter could be associated with an intervalence charge-transfer transition.

The expected paramagnetism of the monoanion is supported by magnetic susceptibility measurements. Solid samples of the sodium and tetraphenylarsonium salts had room-temperature magnetic moments of 1.3 ± 0.1 and 1.7 ± 0.1 μ_B, respectively, when measured at 5 kG by the Gouy method. However, we were unable to obtain an ESR signal under any of the following conditions: (1) electrochemically generated dichloromethane solutions of the monoanion at ambient or low (−160 °C) temperatures; (2) the powdered sodium and tetraphenylarsonium salts at ambient temperatures or in various glasses at ambient or low (−160 °C) temperatures.[17]

Acknowledgment. We thank the National Science Foundation (Grant CHE79-09233) and the Indiana Elks (administered through the Purdue University Cancer Center) for research support and the SOHIO Co. for a Research Fellowship to J.E.A. We also thank Ann T. McKenzie for assistance in the crystal structure determination and Dr. Thomas J. Smith, Kalamazoo College, for measuring the magnetic susceptibility of $Os_2(\mu\text{-}O)(\mu\text{-}O_2CCH_3)_2Cl_4(PPh_3)_4$ by the Faraday method.

Registry No. $Os_2(\mu\text{-}O)(\mu\text{-}O_2CCH_3)_2Cl_4(PPh_3)_2\cdot(C_2H_5)_2O$, 81282-99-7; $Os_2(\mu\text{-}O)(\mu\text{-}O_2CC_2H_5)_2Cl_4(PPh_3)_2$, 84960-56-5; $Os_2(\mu\text{-}O)(\mu\text{-}O_2CCH_3)_2Cl_4(PEt_2Ph)_2$, 84960-57-6; $Os_2(\mu\text{-}O)(\mu\text{-}O_2CCH_3)_2Br_4(PPh_3)_2$, 84960-58-7; $Os_2(\mu\text{-}O)(\mu\text{-}O_2CC_2H_5)_2Br_4(PPh_3)_2$, 84960-59-8; $Ph_4As[Os_2(\mu\text{-}O)(\mu\text{-}O_2CCH_3)_2Cl_4(PPh_3)_2]$, 84960-61-2; $OsO_2Cl_2(PPh_3)_2$, 66984-36-9; $OsO_2Cl_2(PEt_2Ph)_2$, 84960-62-3; $OsO_2Br_2(PPh_3)_2$, 81240-84-8.

Supplementary Material Available: Figures showing the crystal packing in the unit cell and the complete crystal structure with the numbering scheme and tables giving a listing of all bond lengths, bond angles, thermal parameters, and observed and calculated structure factors (36 pages). Ordering information is given on any current masthead page.

---

[17] Attempts are under way to grow single crystals of $Ph_4As[Os_2(\mu\text{-}O)(\mu\text{-}O_2CCH_3)_2Cl_4(PPh_3)_2]$ in order to determine the crystal structure of this salt. Until this is done, we defer further discussion of the spectroscopic and magnetic properties of this complex.

Contribution from the Materials Science Center and the Department of Chemistry,
Cornell University, Ithaca, New York 14853

Stereochemistry of $R_2PX_2^-$ Ligands ($X_2 = S_2$, OS, or O_2) in Molybdenum(II) Dimers and Polymers. A Facile Isomerization about the $Mo\overset{4}{—}Mo$ Core

JOHST H. BURK, GEORGE E. WHITWELL II, JOHN T. LEMLEY, and JAMES M. BURLITCH*

Received July 9, 1982

Stoichiometric reactions of $K_4Mo_2Cl_8$ with MS_2PR_2 (M = K or Na; R = C_2H_5 or C_6H_5) in aqueous methanolic media yielded green, diamagnetic tetrakis((diorganophosphino)dithioato)dimolybdenum(II) species, $Mo_2(S_2PR_2)_4$, characterized by analysis and by IR, NMR, and UV-visible spectroscopy. The diphenyl derivative was also synthesized from the reaction of $Mo_2(OAc)_4$ with excess $(C_6H_5)_2PS_2H$ in diglyme. An X-ray crystal structure analysis of $Mo_2(S_2PEt_2)_4$ revealed the presence of two bridging and two chelating (diethylphosphino)dithioato groups coordinated with virtual C_{2v} symmetry to the Mo_2 core having a Mo–Mo separation of 2.137 (1) Å. The complex crystallizes from toluene and hexane in the triclinic space group $P\bar{1}$ with $a = 11.543$ (1) Å, $b = 14.526$ (1) Å, $c = 11.293$ (1) Å, $\alpha = 92.03$ (1)°, $\beta = 107.33$ (1)°, $\gamma = 85.82$ (1)°, and $Z = 2$. Two Lewis base adducts of $Mo_2(S_2PEt_2)_4$ have also been isolated. The THF complex, $Mo_2(S_2PEt_2)_4\cdot THF$, is a tetrabridged isomer of the preceding compound with virtual D_{4h} symmetry and crystallizes from THF solution in space group $P\bar{1}$ with $a = 10.722$ (1) Å, $b = 9.741$ (2) Å, $c = 10.356$ (1) Å, $\alpha = 108.71$ (1)°, $\beta = 116.79$ (1)°, $\gamma = 79.88$ (1)°, and $Z = 1$. The structure, refined to a residual $R = 0.044$, displays a Mo–Mo bond length of 2.123 (1) Å and a single axially coordinated THF molecule with a Mo–O distance of 3.017 (12) Å. The analogous pyrazine complex, $Mo_2(S_2PEt_2)_4\cdot C_4H_4N_2$, crystallizes from toluene and is found to be isomorphous with $Mo_2(S_2PEt_2)_4\cdot THF$ by X-ray powder diffraction. The novel equilibrium between the two isomers of $Mo_2(S_2PEt_2)_4$ was investigated by ^{31}P NMR spectroscopy and appears to be the first such equilibrium reported for a Mo_2^{4+} system. In noncomplexing solvents, the C_{2v} isomer is favored by 5:2, while in THF the concentrations of the two isomers are approximately equal. Tetrakis((diethylphosphino)thioato)dimolybdenum(II), $Mo_2(SOPEt_2)_4$, and the bis(dialkylphosphinato)molybdenum(II) compounds. $[Mo(O_2PRR')_2]_x$ (R = R′ = *n*-octyl or C_6H_5; R = Me and R′ = C_6H_5) were all prepared by metathesis between $K_4Mo_2Cl_8$ and the potassium salts of $SOPEt_2^-$ or $O_2PRR'^-$, respectively. The first was isolated as a THF monoadduct and found to be tetrabridged by ^{31}P NMR spectroscopy and a partial X-ray single-crystal structure determination. The last three are polymeric, weakly paramagnetic materials in which the molybdenum(II) ions are separated and probably in distorted octahedral environments.

Introduction

As part of a program of study of low-dimensional synthetic metals we have been searching for a family of metal-bridging ligands that would promote the formation of infinite, linear, multiply bonded metal chains. Some potentially interesting systems employed dialkylphosphinato, (dialkylphosphino)thioato, or (dialkylphosphino)dithioato ligands and the quadruply bonded Mo_2^{4+} species; the former are known to act as three-atom bridges[1,2] and the latter is known for its multiply

---

* To whom correspondence should be addressed at the Department of Chemistry.

[1] Cavell, R. G.; Day E. D.; Byers, W.; Watkins, P. M. *Inorg. Chem* .**1972**, *11*, 1759.

0020-1669/83/1322-1306$01.50/0

bonded nature and the availability of axial coordination.[3,4]

The preference of the (diorganophosphino)dithioato ion, $R_2PS_2^-$, for forming four-membered chelate rings with metals is well-known[5] and is exemplified by the monomeric complex $Ni(S_2PMe_2)_2$ which exhibits a square-planar stereochemistry about the metal.[6] The presence of both chelating and catenating (diethylphosphino)dithioato groups in the dimeric complex $[Zn(S_2PEt_2)_2]_2$, shown by X-ray structure analysis,[7] demonstrated the ability of this bidentate ligand to act as a three-atom bridging group between metal centers. Study of complexes of the (dialkylphosphino)dithioato ion with Mo_2^{4+} was of special interest in regard to the question of whether the short metal-metal bond length in the dimolybdenum(II) unit might influence the stereochemical preference of this ligand, given that a large variety of quadruply bridged complexes of Mo_2^{4+} are known.[3,4,8-10]

The multitude of polymeric metal phosphinates which have been synthesized attest to the propensity of the diorganophsophinate ion, $R_2PO_2^-$, to act as a three-atom bridging group between metal centers in preference to chelation.[2] The great practical interest in some of the poly(metal phosphinates) is based on their high degree of polymerization, thermal stability, and plastic properties.

Prior to our work, only two reports of (diorganophosphino)dithioato derivatives of Mo(II) were available. McDonald, Corbin, and Newton described the formation of the monomeric, diamagnetic complex *cis*-$Mo(CO)_2[S_2P(i\text{-}Pr)_2]_2$.[11] Steele and Stephenson tentatively identified the product of the reaction of (diphenylphosphino)dithioic acid with dimolybdenum tetraacetate as $Mo(S_2PPh_2)_2$.[12] Stephenson, Bannister, and Wilkinson prepared $[Mo(O_2PPh_2)_2]_x$ from $Mo(CO)_6$ and HO_2PPh_2, a method analogous to that applied to tetrakis(carboxylato)dimolybdenum(II) syntheses.[13] This paper describes the synthesis and some properties of $Mo_2(S_2PPh_2)_4$ and $Mo_2(S_2PEt_2)_4$ and the tetrahydrofuran and pyrazine adducts of the latter. The crystal and molecular structures of $Mo_2(S_2PEt_2)_4$ and $Mo_2(S_2PEt_2)_4$·THF are presented as well as the results of a ^{31}P NMR study of the novel isomerization of $Mo_2(S_2PEt_2)_4$ in solution. The preparations and characterizations of $Mo_2(SOPEt_2)_4$·THF and the polymeric complexes $[Mo(O_2PPh_2)_2]_x$, $[Mo(O_2PPhMe)_2]_x$, and $[Mo(O_2POct_2)_2]_x$ are described.

Experimental Section

Reactions and other operations employing air-sensitive materials were carried out under argon. The apparatus and techniques have been previously described in detail.[14] Weighing and preparation of analytical and spectroscopic samples of oxidation-sensitive solids were done in a drybox (Vacuum Atmospheres Corp.) under prepurified nitrogen. Melting points were observed in sealed capillaries under argon. Dimolybdenum tetraacetate,[13] $K_4Mo_2Cl_8$,[15] $(NH_4)_5Mo_2Cl_9{\cdot}H_2O$,[16] $Na^+Et_2PS_2^-{\cdot}2H_2O$ (mp 122–124 °C),[17] Et_2POSH,[18-20] and Ph_2PS_2H (mp 57–58 °C)[21] were prepared by known methods. The potassium salts of Et_2POSH, Ph_2PO_2H (Pennwalt), $PhMePO_2H$ (Pennwalt), and Oct_2PO_2H (Pennwalt) were prepared in situ from the free acid and a stoichiometric quantity of K_2CO_3 in methanol and water mixtures or in anhydrous methanol.

Infrared spectra were recorded on a Perkin-Elmer Model 337 spectrophotometer. Electronic spectra were obtained with a Cary Model 2199 spectrophotometer. ^1H NMR spectra were recorded on a Varian Associates Model A-60A/D spectrometer. ^{31}P NMR spectra were obtained with a Bruker Model WM300 spectrometer. Raman spectra were recorded on a Spex 1401 monochromator with a Coherent 500K Kr laser. A slit width of 0.4 mm was used to produce a band-pass of 4.7 cm^{-1}. Data collection was performed by a microprocessor operating in a photon-counting mode. Reported frequencies are accurate to ±1 cm^{-1}. Molecular weights were determined in toluene at 37 °C with a Mechrolab Model 301-A osmometer calibrated with benzil. Microanalyses were performed by the Pascher Microanalytical Laboratory, Bonn, West Germany or by Galbraith Laboratories, Knoxville, TN.

Magnetic measurements were made on a Faraday balance previously described.[22] Samples were sealed in quartz tubes under nitrogen. Approximate magnetic moments were estimated from the room-temperature susceptibility by using the Curie law. A typical plot of uncorrected susceptibility vs. temperature n the range 4–285 K is shown in Figure 3 (supplementary material).

$Mo_2(S_2PEt_2)_4$. A stirred suspension of $K_4Mo_2Cl_8$ (0.632 g, 1.0 mmol) in anhydrous methanol (100 mL) was added dropwise to a degassed solution of $Et_2PS_2^-Na^+{\cdot}2H_2O$ (0.849 g, 4.0 mmol) in water and methanol (50 mL, 1:1) in a Schlenk reaction vessel (SRV) with stirring over a period of 0.75 h. The resulting blue-green suspension was stirred for an additional 4 h. The dark turquoise solid was filtered and washed with a water and methanol mixture (1:1) and anhydrous methanol and then dried under vacuum. The crude $Mo_2(S_2PEt_2)_4$ (0.67 g, 83%) was soluble in tetrahydrofuran, toluene, diglyme, and chlorinated solvents and only slightly soluble in methanol and hexane. Substitution of $(NH_4)_5Mo_2Cl_9{\cdot}H_2O$ for $K_4Mo_2Cl_8$ in the above reaction produced an identical product. Recrystallization from toluene and hexane at −35 °C gave dark green, acicular crystals of $Mo_2(S_2PEt_2)_4$, mp 159–160.5 °C dec. ^1H NMR analysis of the complex in solution showed that a trace of toluene was retained in the crystals. ^1H NMR ($CDCl_3$): δ 1.35 (m, 12 H), 2.52 (m, 8 H), and 7.20 (0.63 H). Anal. Calcd for $C_8H_{20}MoP_2S_4$: C, 23.88; H, 5.01; S, 31.87; mol wt, 804. Found: C, 25.14; H, 5.09; S, 31.25; mol wt (5.5 mM), 708. Recrystallization from diglyme and methanol yielded emerald green crystals of $Mo_2(S_2PEt_2)_4$, mp 160.5–162 °C dec. Anal. Found: C, 24.10; H, 5.03; S, 31.79. IR (KBr pellet): 2954 (m–s), 2919 (m), 2888 sh, 2862 (m–w), 1452 (m), 1400 (m–w), 1377 (m–w), 1255 (w), 1222 (w), 1037 (m), 1026 sh, 1000 (w), 760 (s), 741 sh, 708 (m–s), 672 (m–s), 598 (m–s), 503 sh, and 490 (m) cm^{-1}.

Crystalline $Mo_2(S_2PEt_2)_4$ is moderately air sensitive and turns gray-brown after several days in dry air; in solution, decomposition occurs within 0.5 h. Heating a solution of $Mo_2(S_2PEt_2)_4$ in diglyme or toluene over 100 °C caused thermal decomposition.

$Mo_2(S_2PEt_2)_4$·THF. Cooling a saturated THF solution of $Mo_2(S_2PEt_2)_4$ to −5 °C produced blue-green prismatic crystals. Anal. Calcd for $Mo_2S_8P_4C_{20}H_{48}O$: C, 27.39; H, 5.52; Mo, 21.88; S, 29.25. Found: C, 27.43; H, 5.44; Mo, 22.08; S, 29.47. IR (KBr pellet): 2942 (m–s), 2908 (m–s), 2883 sh, 2853 (m), 1455 (s), 1423 sh, 1400 (m), 1375 (m), 1342 sh, 1255 (m–w), 1220 (m–w), 1036 (m–s), 1026 (m), 1002 (w), 754 (s), 744 (s), 706 (m–s), 668 (s), 595 (s), 503 (m–s), and 487 (m–s) cm^{-1}.

$Mo_2(S_2PEt_2)_4{\cdot}C_4H_4N_2$. This adduct was prepared from $Mo_2(S_2PEt_2)_4$ by precipitation from a toluene solution containing a 40-fold excess of pyrazine (Aldrich; Gold Label) and recrystallized from

---

(2) Block, B. P. *Inorg. Macromol. Rev.* **1970**, *1*, 115.
(3) Cotton, F. A.; Walton, R. F. "Multiple Bonds Between Metal Atoms"; Wiley-Interscience: New York, 1982, pp 84–136.
(4) Templeton, J. L. *Prog. Inorg. Chem.* **1979**, *26*, 211–300.
(5) Kuchen, W.; Hertel, H. *Angew. Chem., Int. Ed. Engl.* **1969**, *8*, 89.
(6) Jones, P. E.; Ansell, G. B.; Katz, L. *J. Chem. Soc., Chem. Commun.* **1968**, 78.
(7) Calligaris, M.; Nardin, E.; Ripamonti, A. *J Chem. Soc. A* **1970**, 714; *J. Chem. Soc., Chem. Commun.* **1968**, 1014.
(8) Cotton, F. A.; Lay, D. G.; Millar, M. *Inorg. Chem.* **1978**, *17*, 186.
(9) Cotton, F. A. *Chem. Soc. Rev.* **1975**, *4*, 27; *Acc. Chem. Res.* **1978**, *11*, 225.
(10) Stiefel, E. I. *Prog. Inorg. Chem.* **1977**, *22*, 141.
(11) McDonald, J. W.; Corbin, J. L.; Newton, W. E. *J. Am. Chem. Soc.* **1975**, *97*, 1970.
(12) Steele, D. F.; Stephenson, T. A. *Inorg. Nucl. Chem. Lett.* **1973**, *9*, 777.
(13) Stephenson, T. A.; Bannister, E.; Wilkinson, G. *J. Chem. Soc.* **1964**, 2538.
(14) Burlitch, J. M. "How to Use Ace No-Air Glassware", Bulletin No. 570; Ace Glass Co.: Vineland, NJ, 1970.
(15) Brencic, J. V.; Cotton, F. A. *Inorg. Chem.* **1970**, *9*, 351.
(16) Brencic, J. V.; Cotton, F. A. *Inorg. Chem.* **1970**, *9*, 346.
(17) Kuchen, W.; Strolenberg, K.; Metten, J. *Chem. Ber.* **1963**, *96*, 1733.
(18) Kuchen, W.; Strolenberg, K.; Metten, J. *Chem. Ber.* **1963**, *96*, 1733.
(19) Borecki, Cz.; Michalski, J.; St. Musicrowicz, J. *J. Chem. Soc.* **1958**, 4081.
(20) Kabachnik, M. I.; Mastrynkova, T. A.; Shipop, A. E.; Melentyeva, T. A. *Tetrahedron* **1960**, *9*, 10.
(21) Higgins, W. A.; Vogel, P. W.; Craig, W. G. *J. Am. Chem. Soc.* **1955**, *77*, 1864.
(22) Kulik, J. D.; Scott, J. C. *J. Vac. Sci. Technol.* **1978**, *15*, 800.

toluene to yield blue-green prismatic crystals. Anal. Calcd for $Mo_2S_8P_4C_{20}H_{48}N_2$: C, 27.21; H, 5.02; N, 3.17. Found: C, 27.35; H, 5.08; N, 3.14. IR (KBr pellet): 3042 (w), 2946 (m–s), 2918 (m–s), 2875 (m), 2857 (m), 1450 (m–s), 1416 (m), 1402 sh, 1376 (m), 1260 (w), 1220 (w), 1158 (w), 1132 (w), 1050 (w), 1036 sh, 1024 (s), 1010 sh, 794 (w), 749 (s), 706 (m–s), 670 (m–s), 599 (m–s), and 492 (m) cm^{-1}.

The THF and pyrazine complexes are monoadducts and are isomorphous as demonstrated by elemental analysis, X-ray powder diffraction, and the single-crystal X-ray structure analysis of $Mo_2(S_2PEt_2)_4$·THF.

$Mo_2(S_2PPh_2)_4$ (Method A). A solution of $Mo_2(O_2CCH_3)_4$ (0.250 g, 0.584 mmol) in diglyme (260 mL) was added without stirring in four portions over a period of 2 days to a solution of Ph_2PS_2H (1.17 g, 4.67 mmol) in diglyme (25 mL) in an SRV. Addition of the first portion resulted in immediate formation of a clear burgundy red mixture. The vessel stood in the dark at room temperature, and after 2 days, growth of clusters of small acicular crystals was observed. Crystal growth was not enhanced by cooling, and after 21 days, the supernatant was decanted and the dark green crystals (8.3 mg) were collected; mp 223–224.5 °C dec. Anal. Calcd for $Mo_2S_8P_4C_{48}H_{40}$: C, 48.48; H, 3.39; S, 21.57. Found: C, 48.28; H, 3.53; S, 21.51. IR (KBr pellet): 3040 (m–w), 2900 (w), 2315 (w), 1480 (w), 1440 (m–w), 1302 (w), 1256 (w), 1183 (w), 1097 (s), 1026 (w), 998 (w), 744 (m–w), 705 sh, 691 (s), 631 (w), 612 (w), 567 sh, 555 (s), and 490 (m–w) cm^{-1}.

$Mo_2(S_2PPh_2)_4$ (Method B). Potassium (diphenylphosphino)dithioate was prepared by the addition of (diphenylphosphino)dithioic acid (1.0 g, 4.0 mmol) and potassium carbonate (0.276 g, 2.0 mmol) to a methanol–water mixture (50 mL, 5:1) with stirring at room temperature, which caused clearing of the mixture with gas evolution; the solution was boiled for 15 min and degassed prior to addition of a stirred suspension of $K_4Mo_2Cl_8$ (0.632 g, 1.0 mmol) in methanol. The crude $Mo_2(S_2PPh_2)_4$ was isolated by filtration as a green solid and washed with a methanol and water mixture, anhydrous methanol, and diethyl ether. The combined filtrate and washings contained 97% of the expected chloride as shown by titration (Volhard method). The dark green solid was dried under vacuum to yield 0.95 g (80%) of crude $Mo_2(S_2PPh_2)_4$, mp 222–224 °C dec. IR (KBr pellet): 3039 (m–w), 2900 (w), 2320 (w), 1480 (w), 1440 (m–w), 1302 (w), 1253 (w), 1180 (w), 1093 (s), 1022 (w), 997 (w), 739 (m), 702 sh, 687 (s), 631 (m–w), 609 (m–w), 565 sh, 553 (s), and 480 (m–w) cm^{-1}. The powder turned dark gray after several days in dry air. It was insoluble in all common organic solvents tried, except for pyridine in which it decomposed.

$Mo_2(SOPEt_2)_4$·THF. This adduct was prepared in the same manner as the dithio analogue. Recrystallization from a mixture of THF and hexane at −35 °C gave fine dark green needlelike crystals, mp 197–200 °C dec. Anal. Calcd for $C_{20}H_{48}Mo_2S_4P_4O_5$: C, 29.56; H, 5.95; S, 15.78; O, 9.84. Found: C, 30.00; H, 6.03; S, 15.20; O, 9.73. ^1H NMR ($CDCl_3$): δ 1.36 (doublet of triplets 12 H), 1.97–3.02 (m, 8 H), 1.86 (m, 2 H), and 3.75 (m, 2 H). ^{31}P NMR (C_7D_8): δ −12.96 (s) and weak, broad resonances due to partial decomposition at δ −2.2, −8.3, and −13.5. IR (Nujol mull): 2940 (s), 2915 (s), 2855 (s), 1465 (m–s), 1457 (m–s), 1437 sh, 1400 (w), 1375 (m), 1362 sh, 1261 (w), 1226 (w), 1050 sh, 1041 sh, 1034 (s), 1009 (m), 1000 (m–w), 981 (w), 963 (w), 890 (w), 767 (m–s), 756 (m–s), 712 (m–w), 668 (m), 655 sh, 574 (m–s), 539 (w), and 463 (m) cm^{-1}.

$[Mo(O_2PPh_2)_2]_x$. This complex was prepared by a literature method[13] from $Mo(CO)_6$ and HO_2PPh_2 and from $K_4Mo_2Cl_8$ and $K^+O_2PPh_2^-$ as described above. The product was a slightly air-sensitive, salmon pink powder that was thermally very stable and insoluble in common organic solvents and water. Anal. Calcd for $C_{24}H_{20}MoO_4P_4$: C, 54.36; H, 3.80; Mo, 18.09; O, 12.07. Found: C, 52.99; H, 3.73; Mo, 18.01; O, 12.05. IR (Nujol mull): 3032 (m), 1478 sh, 1468 (m–s), 1460 (m–s), 1451 sh, 1437 (s), 1379 (m), 1364 sh, 1336 (w), 1185 (w), 1132 (s), 1111 (m–s), 1093 sh, 1057 (m), 1033 (m), 1009 (sh), 1004 (s), 994 sh, 988 (s), 922 (w), 753 (m), 725 (s), 695 (s), 562 (s), 587 (w), 534 (s), 490 (m), and 426 (w) cm^{-1}. Magnetic moment: $\mu_{eff} = 2.0\ \mu_B$/Mo atom.

$[Mo(O_2PPhMe)_2]_x$. As described above, this complex was prepared from $K_4Mo_2Cl_8$ and $K^+MePhPO_2^-$ and isolated as a light red powder that was insoluble in common organic solvents and water. It was somewhat more air sensitive and less thermally stable than $[Mo(O_2PPh_2)_2]_x$. Anal. Calcd for $C_{14}H_{16}MoO_4P_2$: C, 41.40; H, 3.97; Mo, 23.62; O, 15.76. Found: C, 41.22; H, 4.04; Mo, 22.29; O, 15.96. IR (Nujol mull): 3048 (m–w), 1485 sh, 1470 (s), 1441 (m–s), 1417 (m), 1389 (m), 1368 sh, 1291 (m), 1180 (vw), 1131 (s), 1115 (s), 1087 (m–s), 1067 (m), 1035 (s), 1022 (s), 1011 (s), 997 (s), 928 (w), 884 (s), 870 sh, 771 (m), 767 sh, 736 (s), 723 (sh), 702 (m), 693 (m), 620 (vw), 524 (s), 502 (s), 476 (m), and 455 (m–w) cm^{-1}. Magnetic moment: $\mu_{eff} = 1.0\ \mu_B$/Mo atom.[23]

$[Mo(O_2POct_2)_2]_x$. In an analogous preparation, this complex was prepared from $K_4Mo_2Cl_8$ and $K^+Oct_2PO_2^-$ in anhydrous methanol and isolated as a hard, waxy, dark red solid. Attempts to obtain reproducible molecular weight data by using vapor pressure osmometry on deep red, highly viscous solutions of this very air-sensitive material in toluene were unsuccessful due to decomposition in the apparatus. Anal. Calcd for $C_{32}H_{68}MoP_2O_4$: C, 56.96; H, 10.16; Mo, 14.22; P, 9.18. Found: C, 56.32; H, 10.14; Mo, 13.80; P, 9.11. IR (Nujol mull): 1466 (s), 1412 (w), 1383 (m–s), 1375 sh, 1238 (w), 1194 (w), 1120 (s), 1096 (m), 1085 (m), 1070 (m), 1039 (s), 1032 (s), 1007 (m–s), 1002 (s), 837 sh, 814 (m–w), 723 (m–w), and 513 (m) cm^{-1}. Magnetic moment: $\mu_{eff} = 0.8\ \mu_B$/Mo atom.

^{31}P NMR Spectroscopy. Solutions of $Mo_2(S_2PEt_2)_4$ were prepared at 5–10 mM concentrations in toluene-d_8, acetonitrile-d_3, or chloroform-d_1 or in toluene-d_8 that was subsequently diluted with an equal volume of THF and sealed in a 10-mm NMR tube, which contained a centered, sealed capillary containing $P(OCH_3)_3$. In order to simplify the ^{31}P NMR signals, broad-band proton decoupling was employed. Because this technique is subject to a nuclear Overhauser effect (NOE) however,[24] a gated decoupling experiment was developed.[25] In this experiment, the decoupler was turned off and, following a 5-s delay, turned back on while the sample was pulsed and a transient collected; then the cycle was repeated. Final spectra were the Fourier transform results of 200–1000 collected transients.

The spectra were collected at temperatures less than 300 K after allowing the sample 1 h to equilibrate. The chloroform solution suffered some decomposition over 12 h. The acetonitrile solution and the THF and the pyrazine complexes in toluene were observed only at 305 K. The low solubility of the complex at low temperature precluded observation of the formation of the D_{4h} isomer at low temperature.

The ^{31}P resonances observed for $Mo_2(S_2PEt_2)_4$ and their assignments are as follows. Toluene: δ −18.30, bridging (D_{4h}); δ −21.92, bridging (C_{2v}-br); δ −52.09, chelating (C_{2v}-ch). THF: δ −19.33 (D_{4h}); δ −22.15 (C_{2v}-br); δ −51.26 (C_{2v}-ch). Acetonitrile: δ −14.8 (D_{4h}); δ −18.2 (C_{2v}-br); δ −48.1 (C_{2v}-ch). Assignments are predicted by the theory of McConnell[26] concerning diamagnetic anisotropy.

Raman and UV–Vis Spectra. Saturated solutions of $Mo_2(S_2PEt_2)_4$ were prepared in toluene or THF and sealed in 5-mm NMR tubes. The solution of $Mo_2(S_2PEt_2)_4 \cdot C_4H_4N_2$ in toluene was 50 mM. Laser radiation was 6471 Å. Bands observed were at 346 cm^{-1} (in all), and the pyrazine complex and THF solution had shoulders at 362 cm^{-1}. The Raman spectrum of $[Mo(O_2PPh_2)_2]_x$ (1% in KBr pellet) had bands at 455 (m), 488 sh, and 788 (m) cm^{-1}. Absorption spectra of $Mo_2(S_2PEt_2)_4$ in toluene and THF (0.10 mM) were measured from 710 to 280 nm. In toluene, two bands were observed: $\lambda_{max} = 635$ nm, $\epsilon = 1.0 \times 10^3\ M^{-1}\ cm^{-1}$; $\lambda_{max} = 335$ nm, $\epsilon = 5.7 \times 10^3\ M^{-1}\ cm^{-1}$.

---

(23) The magnetic moment calculated from one particular sample of $[Mo(O_2PPhMe_2)_2]_x$ changed from 0.9 to 0.1 μ_B during the course of storage for 13 months while in a sealed tube.

(24) Noggle, J. H.; Schirmer, R. E. "The Nuclear Overhauser Effect"; Academic Press: New York, 1971.

(25) Fukushima, E.; Roeder, S. B. W. "Experimental Pulse NMR: A Nuts and Bolts Approach"; Addison-Wesley: Reading, MA, 1981.

(26) McConnell, H. M. *J. Chem. Phys.* **1957**, *27*, 226.

(27) (a) Lonsdale, K., Ed. "International Tables for X-ray Crystallography"; Kynoch Press: Birmingham, England, 1969; Vol. I. (b) *Ibid.*, Vol. III, Table 3.3.2C.

(28) DeMeulinae, J.; Tompa, H. *Acta Crystallogr.* **1965**, *19*, 1014.

(29) Alcock, N. W. *Acta Crystallogr., Sect. A* **1969**, *A25*, 518.

(30) Busing, W. R.; Martin, K. O.; Levy, H. A. "OR-FLS, A Fortran Crystallographic Least-Squares Program", Report ORNL-TM-305; Oak Ridge National Laboratory: Oak Ridge, TN, 1962.

(31) Busing, W. R.; Martin, K. O.; Levy, H. A. "ORFFE, A Fortran Crystallographic Function and Error Program", Report ORNL-TM-306; Oak Ridge National Laboratory: Oak Ridge, TN, 1964.

(32) Johnson, C. K. "ORTEP-II, A Fortran Thermal-Ellipsoid Plot Program for Crystal Structure Illustrations", Report ORNL-TM-5138; Oak Ridge National Laboratory: Oak Ridge, TN, 1976.

(33) Stewart, J. M., Ed. "The X-ray System—Version of 1976", Report TR-446 of the Computer Science Center; University of Maryland: College Park, MD, 1976.

Table I. Crystal Data and Details of the Diffraction Experiments

	$Mo_2(S_2PEt_2)_4$ (C_{2v})	$Mo_2(S_2PEt_2)_4 \cdot THF$ (D_{4h})
	(A) Crystal Data	
temp, °C	21 ± 3	18 ± 3
a, Å	11.544 (1)	10.772 (1)
b, Å	14.526 (1)	9.741 (2)
c, Å	11.293 (1)	10.356 (1)
α, deg	92.03 (1)	108.71 (1)
β, deg	107.33 (1)	116.79 (1)
γ, deg	85.82 (1)	79.88 (1)
V, Å^3	1797.2	918.2
F_{000}	816	448
cryst system	triclinic	triclinic
systematic absences	none	none
space group[27a]	$P\bar{1}$ (C_i^1; No. 2)	$P\bar{1}$ (C_i^1; No. 2)
Z	2	1
ρ_{calcd}, g/cm^3	1.49	1.75
ρ_{measd}, g/cm^3	1.57	1.66
mol wt	804.78	876.89
μ, cm^{-1}	13.4[a]	15.4[b]
cryst shape	trapezoidal plate	parallelepiped
cryst dimens, mm	0.24 × 0.32 × 0.08	0.3 × 0.4 × 0.4
	(B) Measurement of Intensity Data	
diffractometer	Picker FACS-1	Syntex $P2_1$
radiation	Mo; Zr filtered	Mo; graphite monochromated
λ, Å	0.710 69	0.710 69
scan type	θ–2θ	ω
scan range, deg	1.5[c]	1.0[c]
scan rate, deg/min	1.0	1.0–20.0[d]
bkgd measmt	stationary; 40 s at each end of scan	0.5° at each end of scan
std reflcns	3 every 50	3 every 50
variation in stds	<3%	<4%
max 2θ, deg; $(\sin\theta)/\lambda$, Å^{-1}	27.5; 0.648	30.0; 0.7035
tot reflcns	8234	5367
unique obsd reflcns	7126 ($F_o \geq 1.58\sigma_F$)	4807 ($F_o^2 \geq 3\sigma_F$)
	(C) Structure Solution and Refinement	
computer	Prime 400[e]	Prime 850[f]
soln method	Patterson and Fourier	Patterson and Fourier
refinement	full-matrix least squares	full-matrix least squares
anisotropic convergence[g]	$R = 0.072$, $R' = 0.093$	$R = 0.044$, $R' = 0.065$
max shifts in final cycle, d/σ	0.26	0.028
error of fit	3.89	0.141
data:parameter	20.1	25.2
max residual electron density in final diff map, e/Å^3	2.69[h]	0.6

[a] Data were corrected for absorption by an algorithm for a model of crystal defined by six faces.[28,29] A dispersion correction was included for Mo.[27b] [b] Absorption correction was not made since the crystal had a quite isotropic shape. Dispersion correction was included for Mo, S, and P.[27b] [c] This included a variable increment to allow for dispersion. [d] Variable scan rate. [e] The programs used on the Prime 400 were OR-FLS,[30] ORFFE,[31] and ORTEP.[32] [f] The programs used on the Prime 850 were XRAY76[33] and ORTEP.[32] [g] $R = \Sigma \lvert F_o\rvert - \lvert F_c\rvert / \Sigma \lvert F_o\rvert$; $R' = (\Sigma(\lvert F_o\rvert - \lvert F_c\rvert)^2 / \Sigma \lvert F_o\rvert^2)^{0.5}$. [h] Five weak uninterpretable peaks were present (near $^1/_2$, $^1/_2$, 0) not near the molecule of interest and were probably due to toluene solvate.

Table II. Fractional Coordinates for $Mo_2(S_2PEt_2)_4$ (C_{2v})

atom	x	y	z
Mo1	0.2275 (1)	0.2451 (1)	0.2644 (1)
Mo2	0.1228 (1)	0.2152 (1)	0.3840 (1)
Mo3	0.2110 (7)	0.2847 (5)	0.3726 (8)
Mo4	0.1846 (7)	0.1517 (6)	0.2885 (7)
S1	0.4184 (2)	0.3139 (2)	0.3966 (2)
S2	0.3816 (2)	0.1100 (2)	0.2688 (3)
S3	0.2437 (2)	0.2583 (2)	0.6046 (2)
S4	0.1926 (3)	0.0571 (2)	0.4811 (2)
S5	−0.0476 (2)	0.1305 (2)	0.2437 (2)
S6	0.1149 (2)	0.1770 (2)	0.0577 (2)
S7	−0.0134 (2)	0.3584 (2)	0.3745 (2)
S8	0.1498 (2)	0.4040 (2)	0.1885 (2)
P1	0.5001 (2)	0.1865 (2)	0.3948 (2)
P2	0.2152 (3)	0.1281 (2)	0.6418 (3)
P3	−0.0539 (2)	0.1754 (2)	0.0749 (2)
P4	0.0848 (2)	0.4527 (2)	0.3282 (2)
C1	0.6443 (10)	0.1922 (9)	0.3597 (12)
C2	0.6311 (14)	0.2377 (14)	0.2386 (15)
C3	0.5369 (11)	0.1318 (8)	0.5463 (10)
C4	0.6117 (14)	0.1922 (12)	0.6516 (12)
C5	0.0884 (12)	0.1241 (9)	0.7054 (13)
C6	−0.0332 (12)	0.1698 (10)	0.6166 (15)
C7	0.3464 (12)	0.0743 (9)	0.7651 (11)
C8	0.3793 (13)	0.1311 (12)	0.8856 (12)
C9	−0.1417 (10)	0.0977 (8)	−0.0429 (10)
C10	−0.2670 (12)	0.0836 (10)	−0.0303 (12)
C11	−0.1366 (9)	0.2879 (7)	0.0457 (9)
C12	−0.1404 (13)	0.3286 (9)	−0.0796 (11)
C13	−0.0093 (11)	0.5597 (7)	0.2842 (10)
C14	−0.1223 (15)	0.5475 (10)	0.1703 (13)
C15	0.2088 (10)	0.4856 (8)	0.4658 (10)
C16	0.2857 (15)	0.5576 (10)	0.4405 (15)

Table III. Bond Distances (Å) in $Mo_2(S_2PEt_2)_4$ (C_{2v})

Mo1–Mo2	2.137 (1)	S5–P3	2.015 (4)
Mo3–Mo4	2.124 (11)	S6–P3	2.017 (4)
Mo1–S1	2.518 (2)	S7–P4	2.017 (4)
Mo1–S2	2.541 (3)	S8–P4	2.025 (4)
Mo1–S6	2.518 (2)	S–P av br	2.018
Mo1–S8	2.499 (2)	S–P av ch	2.018
Mo2–S3	2.548 (2)	P1–C1	1.831 (13)
Mo2–S4	2.551 (3)	P1–C3	1.831 (12)
Mo2–S5	2.502 (2)	P2–C5	1.818 (16)
Mo2–S7	2.498 (2)	P2–C7	1.868 (12)
Mo–S av br	2.504	P3–C9	1.825 (11)
Mo–S av ch	2.540	P3–C11	1.820 (10)
Mo3–S1	2.396 (9)	P4–C13	1.824 (11)
Mo3–S3	2.572 (9)	P4–C15	1.847 (10)
Mo3–S7	2.735 (8)	P–C av	1.833
Mo3–S8	2.651 (8)	C1–C2	1.502 (23)
Mo4–S2	2.383 (9)	C3–C4	1.535 (18)
Mo4–S4	2.589 (9)	C5–C6	1.577 (17)
Mo4–S5	2.615 (8)	C7–C8	1.528 (19)
Mo4–S6	2.521 (8)	C9–C10	1.525 (19)
S1–P1	2.017 (3)	C11–C12	1.540 (17)
S2–P1	2.021 (3)	C13–C14	1.551 (17)
S3–P2	2.023 (4)	C15–C16	1.508 (22)
S4–P2	2.013 (4)	C–C av	1.533

In THF, a third band was also present: $\lambda_{max} = 636$ nm, $\epsilon = 8.5 \times 10^2$ M^{-1} cm^{-1}; $\lambda_{max} = 334$ nm, $\epsilon = 6.4 \times 10^3$ M^{-1} cm^{-1}; $\lambda_{max} = 295$ nm, $\epsilon = 3.5 \times 10^3$ M^{-1} cm^{-1}.

Crystal Structure Determinations. The crystal data and crystallographic experimental details are presented in Table I. Both structures were solved and refined in routine fashion using Patterson and Fourier syntheses and full-matrix least-squares refinement. Each structure presents a small degree of disorder, which was discovered in both cases by difference Fourier synthesis. In the crystal structure of the C_{2v} isomer, a second pair of Mo atoms was found at approximately right angles to the first pair. Inclusion of this second pair of Mo atoms with an occupancy factor of 0.073 (mutually exclusive with the first pair) in the refinement led to a standard residual of 7.2%; prior to this addition, R was 10%. The final values of the positional and thermal parameters for $Mo_2(S_2PEt_2)_4$ (C_{2v}) are presented in Table II. Selected interatomic distances and angles are presented in Tables III and IV, respectively. Stereoscopic drawings of the major and minor forms of $Mo_2(S_2PEt_2)_4$ are presented in Figure 1.

A second crystal habit in space group $P\bar{1}$ was occasionally observed for $Mo_2(S_2PEt_2)_4$ crystallized from toluene and hexane mixtures. The unit cell dimensions were $a = 11.581$ (3) Å, $b = 11.728$ (5) Å, $c = 6.674$ (2) Å, $\alpha = 104.53$ (2)°, $\beta = 98.93$ (2)°, $\gamma = 114.59$ (2)°, and $Z = 1$.

The final values of the positional and thermal parameters for $Mo_2(S_2PEt_2)_4 \cdot THF$ (D_{4h}) are presented in Table V. The interatomic

Table IV. Bond Angles (deg) in $Mo_2(S_2PEt_2)_4$ (C_{2v})

Mo2-Mo1-S1	107.5 (1)	S1-P1-C1	110.6 (4)
Mo2-Mo1-S2	108.4 (1)	S1-P1-C3	111.5 (4)
Mo2-Mo1-S6	104.3 (1)	S2-P1-C1	112.5 (4)
Mo2-Mo1-S8	104.4 (1)	S2-P1-C3	108.7 (4)
Mo1-Mo2-S3	107.6 (1)	C1-P1-C3	106.4 (6)
Mo1-Mo2-S4	110.2 (1)	S3-P2-S4	105.5 (2)
Mo1-Mo2-S5	103.0 (1)	S3-P2-C5	112.4 (4)
Mo1-Mo2-S7	103.1 (1)	S3-P2-C7	112.2 (4)
Mo1-Mo2-S av br	103.7	S4-P2-C5	113.5 (4)
Mo1-Mo2-S av ch	108.4	S4-P2-C7	110.1 (4)
Mo4-Mo3-S1	106.2 (4)	C5-P2-C7	103.4 (6)
Mo4-Mo3-S3	104.8 (4)	S-P-S av ch	106.3
Mo4-Mo3-S7	106.5 (4)	S-P-C av ch	108.8
Mo4-Mo3-S8	106.2 (4)	C-P-C av ch	104.9
Mo3-Mo4-S2	101.1 (4)	S5-P3-S6	110.9 (1)
Mo3-Mo4-S4	99.5 (4)	S5-P3-C9	108.7 (4)
Mo3-Mo4-S5	104.9 (4)	S5-P3-C11	110.4 (4)
Mo3-Mo4-S6	106.1 (4)	S6-P3-C9	109.0 (4)
Mo1-S1-P1	86.2 (1)	S6-P3-C11	112.0 (4)
Mo1-S2-P1	85.4 (1)	C9-P3-C11	105.6 (4)
Mo1-S6-P3	101.0 (1)	S7-P4-S8	110.6 (2)
Mo1-S8-P4	100.2 (1)	S7-P4-C13	109.5 (4)
Mo2-S3-P2	83.5 (1)	S7-P4-C15	110.1 (4)
Mo2-S4-P2	83.7 (1)	S8-P4-C13	110.8 (4)
Mo2-S5-P3	102.3 (1)	S8-P4-C15	111.5 (4)
Mo2-S7-P4	101.1 (1)	C13-P4-C15	104.1 (5)
Mo1,2-S-P av br	101.2	S-P-S av br	110.8
Mo1,2-S-P av ch	84.7	S-P-C av br	110.2
Mo3-S1-P1	103.5 (2)	C-P-C av br	104.8
Mo3-S3-P2	113.2 (2)	P1-C1-C2	113.5 (9)
Mo3-S7-P4	68.2 (2)	P1-C3-C4	112.4 (10)
Mo3-S8-P4	70.0 (2)	P2-C5-C6	112.0 (11)
Mo4-S2-P1	107.0 (2)	P2-C7-C8	113.1 (9)
Mo4-S4-P2	116.5 (2)	P3-C9-C10	113.5 (9)
Mo4-S5-P3	82.2 (2)	P3-C11-C12	113.4 (8)
Mo4-S6-P3	84.7 (2)	P4-C13-C14	113.0 (8)
S1-P1-S2	107.1 (1)	P4-C15-C16	113.8 (9)

Table V. Fractional Coordinates for $Mo_2(S_2PEt_2)_4 \cdot THF$ (D_{4h})

atom	*x*	*y*	*z*
Mo	−0.00293 (3)	−0.01915 (3)	0.09388 (3)
S1	0.0835 (1)	−0.2799 (1)	0.0751 (1)
S2	0.2348 (1)	0.0543 (1)	0.3019 (1)
S3	0.0973 (1)	−0.2180 (1)	−0.2152 (1)
S4	0.2442 (1)	0.1103 (1)	0.0045 (1)
P1	0.0459 (1)	−0.3616 (1)	−0.1445 (1)
P2	0.3509 (1)	0.0381 (2)	0.1898 (1)
C1	0.1483 (9)	−0.5297 (6)	−0.1670 (9)
C2	−0.3026 (11)	0.5216 (10)	0.0700 (16)
C3	−0.1321 (7)	−0.4166 (6)	−0.2607 (7)
C4	0.1714 (11)	0.4603 (10)	0.4327 (8)
C5	0.4221 (6)	−0.1441 (8)	0.1439 (7)
C6	0.4883 (9)	−0.2140 (12)	0.2757 (9)
C7	0.5019 (7)	0.1490 (14)	0.3138 (9)
C8	0.5683 (16)	0.2094 (20)	0.2466 (18)
C9	0.4963 (25)	0.2956 (28)	0.3716 (31)
O1	−0.0172 (9)	−0.1033 (11)	0.3429 (9)
C10	−0.1209 (20)	−0.0192 (25)	0.4181 (20)
C11	−0.0398 (31)	0.0872 (25)	0.5369 (26)
C12	0.1008 (37)	0.0649 (33)	0.5909 (39)
C13	0.1064 (17)	−0.1043 (23)	0.4742 (21)

distances and angles derived from these positions are presented in Tables VI and VII, respectively. A stereoscopic drawing of $Mo_2(S_2PEt_2)_4 \cdot THF$ is presented in Figure 2. The D_{4h} isomer presented a different form of disorder in one ethyl moiety. The methyl carbon atom attached to C7 occupies either of two positions: C8 with an occupancy factor of 0.70 or C9 (represented with dashed lines in Figure 2) with an occupancy factor of 0.30. An additional constraint is imposed on this molecule by the inherent unit cell symmetry, which requires C_i molecular symmetry. Moreover, the complexed THF molecule also sits on a crystallographic inversion center. It has therefore been included with a 0.50 occupancy factor, retaining the $[Mo_2]$:THF formulation.

The crystal structure of $Mo_2(SOPEt_2)_4 \cdot THF$ is quite similar to that of the D_{4h} isomer of $Mo_2(S_2PEt_2)_4 \cdot THF$.[34]

Table VI. Bond Distances (Å) in $Mo_2(S_2PEt_2)_4 \cdot THF$ (D_{4h})

Mo-Mo′	2.123 (1)	P1-C1	1.818 (7)
Mo-S1	2.524 (1)	P1-C3	1.811 (6)
Mo-S2	2.529 (1)	P2-C5	1.809 (7)
Mo-S3′	2.532 (1)	P2-C7	1.818 (9)
Mo-S4′	2.535 (1)	P-C av	1.814
Mo-S av	2.530	C1-C2	1.505 (12)
Mo-O1	3.017 (12)	C3-C4	1.559 (11)
S1-S3	3.319 (2)	C5-C6	1.544 (13)
S2-S4	3.343 (2)	C7-C8	1.485 (27)
S-S av	3.331	C7-C9	1.362 (27)
S1-P1	2.022 (2)	C-C av	1.491
S2-P2	2.015 (2)	O1-C10	1.605 (25)
S3-P1	2.023 (2)	O1-C13	1.412 (17)
S4-P2	2.023 (2)	C10-C11	1.372 (28)
S-P av	2.021	C11-C12	1.361 (47)
		C12-C13	1.713 (35)

Table VII. Bond Angles (deg) in $Mo_2(S_2PEt_2)_4 \cdot THF$ (D_{4h})

Mo′-Mo-S1	103.1 (1)	S3-P1-C3	112.0 (2)
Mo′-Mo-S2	103.1 (1)	S2-P2-C5	112.0 (3)
Mo′-Mo-S3′	104.2 (1)	S2-P2-C7	108.5 (3)
Mo′-Mo-S4′	104.8 (1)	S4-P2-C5	111.3 (2)
Mo-Mo-S av	103.8	S4-P2-C7	108.1 (4)
Mo′-Mo-O1	174.5 (2)	S-P-C av	110.3
S1-Mo-S2	87.8 (1)	C1-P1-C3	103.8 (3)
S1-Mo-S3′	152.6 (1)	C5-P2-C7	104.8 (4)
S1-Mo-S4′	86.8 (1)	C-P-C av	104.4
S2-Mo-S3′	87.1 (1)	P1-C1-C2	116.4 (5)
S2-Mo-S4′	152.1 (1)	P1-C3-C4	113.5 (7)
S3′-Mo-S4′	85.2 (1)	P2-C5-C6	114.2 (5)
Mo-S1-P1	103.1 (1)	P2-C7-C8	118.9 (7)
Mo-S2-P2	103.3 (1)	P2-C7-C9	124.7 (11)
Mo′-S3-P1	101.9 (1)	P-C-C av	117.5
Mo′-S4-P2	102.2 (1)	Mo-O1-C10	121.4 (10)
Mo-S-P av	102.6	Mo-O1-C13	118.5 (12)
S1-P1-S3	110.3 (1)	C10-O1-C13	99.7 (12)
S2-P2-S4	111.8 (1)	O1-C10-C11	102.7 (20)
S-P-S av	111.0	C10-C11-C12	117.7 (24)
S1-P1-C1	108.8 (3)	C11-C12-C13	98.7 (19)
S1-P1-C3	111.8 (3)	O1-C13-C12	102.6 (16)
S3-P1-C1	109.9 (4)		

Results and Discussion

Synthesis and Characterization. The preferred synthesis route to the $[Mo(X_2PR_2)_2]_n$ (n = 2 or x) complexes is described by eq 1. Under these conditions the Mo_2^{4+} complexes

$$\mathrm{K_4Mo_2Cl_8} + 4\mathrm{R_2PX_2^-M^+} \xrightarrow{\mathrm{MeOH/H_2O}} [\mathrm{Mo(X_2PR_2)_2}]_n + 4\mathrm{KCl} + 4\mathrm{MCl} \quad (1)$$

$$\mathrm{M} = \mathrm{Na\ or\ K};\ \mathrm{X_2} = \mathrm{S_2},\ \mathrm{O_2},\ \mathrm{or\ SO};\ \mathrm{R} = \mathrm{Ph\ or\ Et}$$

were obtained as insoluble green powders, and the completeness of the metathetical reaction was monitored by the chloride content of the supernatant liquid. Ligand-exchange reactions in aqueous media with preservation of the dinuclear Mo(II) core have been described.[35] The complexes $Mo_2(S_2PEt_2)_4$ and

---

(34) $Mo_2(SOPEt_2)_4 \cdot THF$ crystallizes from a mixture of THF and hexane in space group *P4nc* (C_{4v}^6; No. 104[27a]), with a = 12.648 (7) Å, b = 12.648 (7) Å, c = 10.510 (1) Å, $\alpha = \beta = \gamma$ = 90.00 (3)°, and Z = 2. The structure was solved by Patterson and Fourier syntheses and refined by full-matrix least squares to a residual of R = 0.145. The experimental and computational procedures were quite similar to those employed in the $Mo_2(S_2PEt_2)_4 \cdot THF$ structure determination. The Mo–Mo vector lies along the fourfold rotation axis of the cell (as does the THF oxygen atom) and is bisected by a horizontal mirror plane; thus one-fourth of a Mo atom and a single $SOPEt_2$ ligand are sufficient to model the structure, which contains four (diethylphosphino)thioato ligands bridging the Mo_2^{4+} core and a single axially coordinated THF molecule. The following molecular dimensions have been calculated: Mo–Mo = 2.128 (2) Å; Mo–O = 2.148 (29) Å; Mo–S = 2.548 (25) Å; Mo–O(THF) = 2.614 (53) Å; S–P = 2.019 (24) Å; O–P = 1.474 (29) Å; O–S(bite) = 2.904 (19) Å; Mo–Mo–O = 100.5 (4)°; Mo–Mo–S = 98.4 (4)°; Mo–O–P = 121.2 (8)°; Mo–S–P = 107.5 (4)°; S–P–O = 112.4 (6)°.

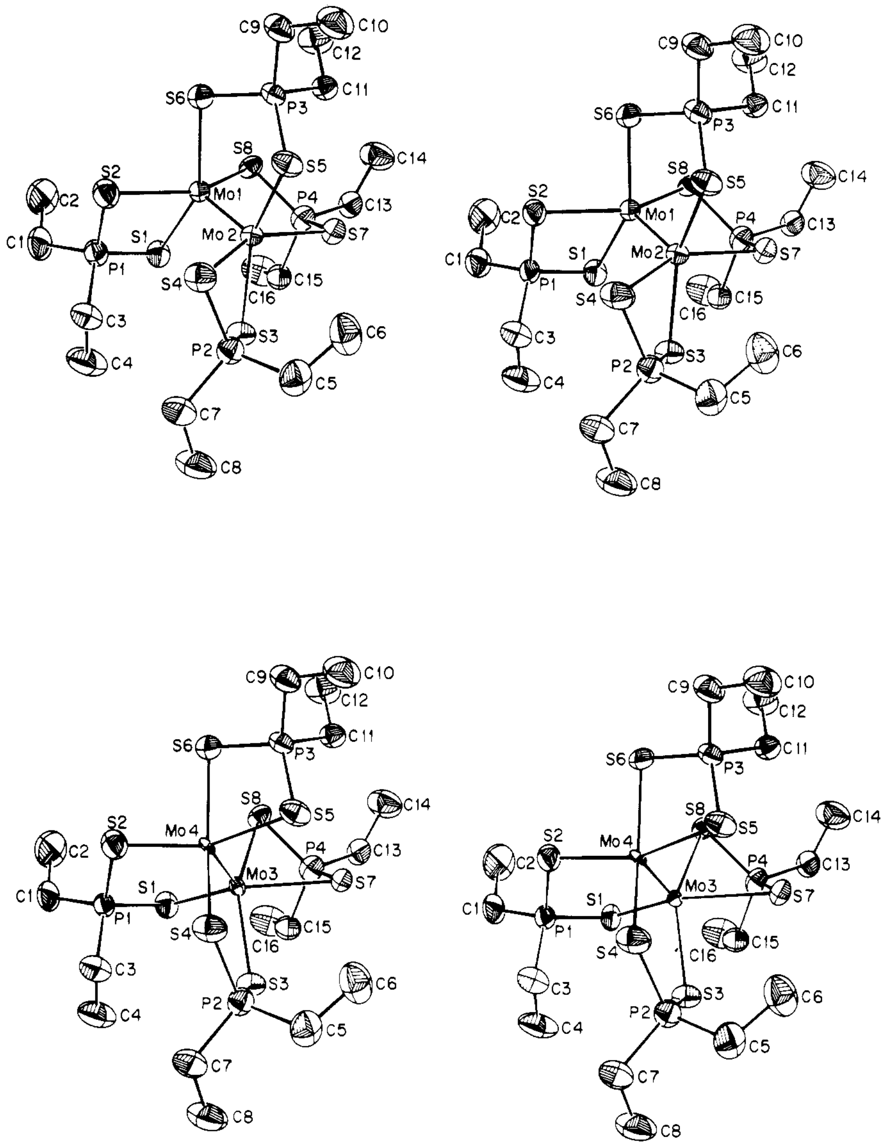

Figure 1. Stereoscopic view of the major (upper) and minor (lower) forms of $Mo_2(S_2PEt_2)_4$ (C_{2v}) with the atoms represented by their 50% probability ellipsoids.

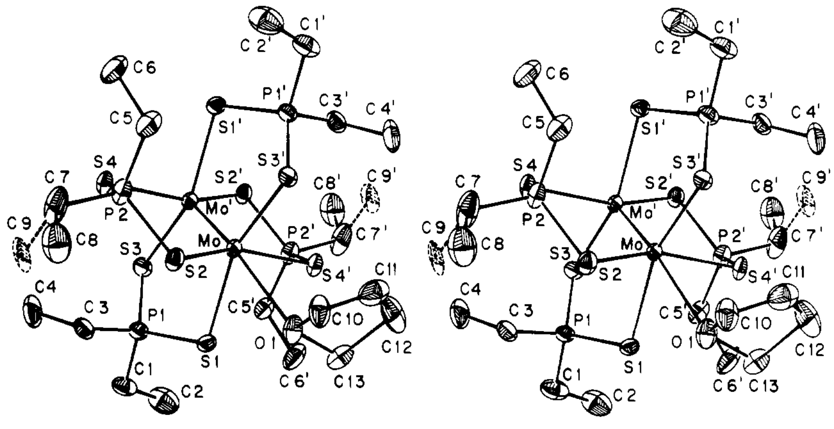

Figure 2. Stereoscopic view of $Mo_2(S_2PEt_2)_4$·THF with the atoms represented by their 50% probability ellipsoids.

$Mo_2(SOPEt_2)_4$ were soluble in various organic solvents and were obtained as slightly air-sensitive, dark green, needlelike crystals upon recrystallization. Their diamagnetic natures were inferred from the sharpness of the peaks in their ^1H NMR spectra. In toluene $Mo_2(S_2PEt_2)_4$ exists as Mo_2L_4 units as shown by molecular weight measurements. Solutions of $Mo_2(S_2PEt_2)_4$ darkened slowly upon standing at room temperature and rapidly when heated. The black decomposition product(s) has (have) not been characterized.

The diamagnetic complex $Mo_2(S_2PPh_2)_4$ is insoluble in water and nearly all organic solvents; attempted recrystallization from diglyme at 140 °C caused extensive thermal decomposition. This limitation notwithstanding, $Mo_2(S_2PPh_2)_4$ was obtained as well-formed single crystals by slow mixing of reactants in warm diglyme solutions according to eq 2. The

---

(35) (a) Bowen, A. R.; Taube, H. *J. Am. Chem. Soc.* **1971**, *93*, 3287. (b) Bowen, A. R.; Taube, H. *Inorg. Chem.* **1974**, *13*, 2245.

$$Mo_2(O_2CCH_3)_4 + \text{excess } Ph_2PS_2H \xrightarrow{\text{diglyme}} Mo_2(S_2PPh_2)_4 + 4CH_3CO_2H \quad (2)$$

IR spectrum of the resulting dark green needlelike crystals of $Mo_2(S_2PPh_2)_4$ was identical with that of the green powder obtained from the reaction of $K_4Mo_2Cl_8$ and $K^+Ph_2PS_2^-$. In contrast to the green, dimeric R_2PS_2 and R_2POS derivatives, the diorganophosphinates are pink or red and display weak paramagnetism. They possess similar or greater air sensitivity but are more thermally stable than their sulfur-containing analogues.

Crystal Structure of $Mo_2(S_2PEt_2)_4$ (C_{2v}). The molecular structure of $Mo_2(S_2PEt_2)_4$ (Figure 1) exhibits virtual C_{2v} symmetry with two (diethylphosphino)dithioato groups bridging the tightly bound Mo_2 core in a cis fashion with a chelating ligand group on each Mo atom completing the distorted square-pyramidal coordination. The Mo–Mo distance (2.137 Å) is intermediate in the range of bond distances reported for quadruply bonded dimolybdenum derivatives[3,4,9,10] and is quite similar to the average Mo–Mo bond length reported for $Mo_2(S_2CCH_3)_4 \cdot 2THF$ and $Mo_2(S_2CC_6H_5)_4 \cdot 2THF$[36] (2.138 Å). It is slightly longer than that of $Mo_2(S_2COC_2H_5)_4 \cdot 2THF$ with 2.125 Å.[37]

The average S–S bite distances are 3.32 and 3.23 Å for the bridging and chelating ligands, respectively, which correspond closely to the 3.37 Å distance found for the dimeric complex $[Zn(S_2PEt_2)_2]_2$.[7] These values are significantly larger than the average bite distance of the bridging dithiocarboxylato ligands with 2.95 and 2.99 Å for the *O*-ethyl carbonato groups in the above complexes. The average Mo–S bond lengths of the chelating and the bridging groups are 2.540 and 2.504 Å, respectively, which may indicate stronger bonding of the latter to the Mo_2 unit despite the larger ligand bite. These Mo–S distances are longer than those observed for the quadruply bridged dithiocarboxylato (2.465 Å) and *O*-ethyl carbonato (2.478 Å) compounds.[36,37]

The shorter Mo–S bonds in $Mo_2(S_2PEt_2)_4$ for the bridging ligands are associated with more obtuse S–P–S angles (mean 110.8°) in the five-membered Mo_2S_2P rings than those found in the four-membered MoS_2P rings (mean 106.3°). Similar shorter M–S bond lengths for bridging vs. chelating Et_2PS_2 groups were observed in the dimeric complex $[Zn(S_2PEt_2)_2]_2$[4] and can be attributed to decreased steric hindrance with larger S–P–S angles in the bridging units.[38,39] The average P–S bond length in the bridging and chelating Et_2PS_2 groups in $Mo_2(S_2PEt_2)_4$ is 2.018 Å, agreeing with values found for $[Zn(S_2PEt_2)_2]_2$ (mean 2.02 Å)[4] and $Ni(S_2PMe_2)_2$ (mean 2.01 Å).[6]

From the drawing (Figure 1), from models of $Mo_2(S_2PEt_2)_4$, and from the demonstrated existence of its tetrabridged isomer (following) it is apparent that steric hindrance due to the ethyl substituents between the bridging (diethylphosphino)dithioato groups cannot account for the mixed stereochemistry. However, the relatively large bite of this ligand may be a factor. The unit cell packing presented no unusual intermolecular contacts.

The crystallographic disorder is attributed to a second pair of molybdenum positions (7.3%) at right angles to the first. Disorder of the same type was previously observed in the structure of $K_4Mo_2Cl_8 \cdot 2H_2O$,[40] as well as for the dirhenium derivatives $(n\text{-}Bu_4N)_2Re_2Cl_8$[41] and $Re_2Cl_4(PEt_3)_4$.[42] The peculiar structural effect of the alternate Mo sites in $Mo_2(S_2PEt_2)_4$ is to exchange the roles of the ligands; i.e., the bridging ligands of the major form become chelating ligands in the minor form and vice versa. While the mixed-bonding mode employed by identical ligands here in $Mo_2(S_2PEt_2)_4$ is unique in dinuclear Mo(II) compounds, the bridged and chelated bis(acetato)(diethylpyrazolylborato)dimolybdenum complex is known.[43] Likewise, $Mo_2(\eta^3\text{-allyl})_4$ displays a similar structure without the formation of four- or five-membered rings by the ligands with the metal.[44]

Crystal Structure of $Mo_2(S_2PEt_2)_4 \cdot THF$ (D_{4h}). The molecular structure of $Mo_2(S_2PEt_2)_4 \cdot THF$ exhibits virtual D_{4h} symmetry (excluding the THF molecule), with all four (diethylphosphino)dithioato ligands bridging the Mo_2 core. The sulfur atoms assume a nearly cubic disposition about the dimetal core (S–S distances 3.41 ± 0.09 Å; S–S–S angle 90 ± 2°). The THF oxygen atom is coordinated at the axial site of one Mo atom. The Mo–Mo distance (2.123 Å) is shorter than that found in the C_{2v} isomer (2.137 Å) and is very similar to the 2.125 Å Mo–Mo distance found in $Mo_2(S_2COC_2H_5)_4 \cdot 2THF$.[37] One expects from empirical grounds[45,46] that axial ligand coordination to quadruply bound metal dimers might cause a slight lengthening of the metal–metal bond. Two factors apparent in this case may explain our observation of the opposite tendency. The two isomers of $Mo_2(S_2PEt_2)_4$ present different overall modes of coordination by the bidentate (diethylphosphino)dithioato ligands, and in fact the shorter Mo–Mo bond is found in the D_{4h} isomer. This indicates that the Mo–Mo bond is strengthened by interaction with the bridging ligands. Additionally, the Mo–O distance (3.017 Å) is very long compared to the bis(tetrahydrofuran) complexes of tetrakis(*O*-ethyl dithiocarbonato)dimolybdenum (2.795 Å), tetrakis(dithiobenzoato)dimolybdenum (2.727 Å), and tetrakis(dithioacetato)dimolybdenum (2.667 Å) and only one such ligand is present per dimolybdenum unit, so the THF oxygen is not contributing significant electron density to the complex. An explanation of the apparent weakness of this Mo–O bond may be found in the comparison of the shortest S···O contact distances found in the above compounds. The shortest S···O contact distance calculated from the reported unit cell and atomic positional parameters[36,37] for $Mo_2(S_2COC_2H_5)_4 \cdot 2THF$ is 3.28 Å, for $Mo_2(S_2CC_6H_5)_4 \cdot 2THF$ it is 3.24 Å, and for $Mo_2(S_2CCH_3)_4 \cdot 2THF$ it is 3.25 Å. The shortest S···O contact distance of 3.29 Å found in $Mo_2(S_2PEt_2)_4 \cdot THF$ compares well with these values. The sum of the van der Waals radii for S and O is 3.13 Å,[47,48] which is in keeping with the postulate that steric interaction between oxygen and sulfur atoms limits the approach of the oxygen atom to the molybdenum atom.

The bites of the (diethylphosphino)dithioato ligands average 3.33 Å, which is close to that found for the bridging phosphinodithioato ligands of the C_{2v} structure (3.32 Å). The average Mo–S distance (2.530 Å) is longer than that found in the bridging ligands of the C_{2v} isomer, a factor which may be related to the associated shorter Mo–Mo distance. The average S–P distance (2.021 Å) is slightly longer than that of the bridging ligands of the C_{2v} isomer (2.018 Å), while the average P–C distance (1.814 Å) is somewhat longer than that

---

(36) Cotton, F. A.; Fanwick, P. E.; Niswander, R. H.; Sekutowski, J. C. *Acta Chem. Scand., Ser. A* **1978**, *A32*, 663.
(37) Ricard, L.; Karagiannidis, P.; Weiss, R .*Inorg. Chem.* **1973**, *12*, 2179.
(38) Coates, G. E.; Mukherjee, R. *J Chem. Soc.* **1964**, 1295.
(39) Kuchen, W.; Metten, J.; Judat, A. *Chem. Ber.* **1964**, *97*, 2306; **1968**, *101*, 1991.
(40) Brencic, J. V.; Cotton, F A. *Inorg. Chem.* **1969**, *8*, 7.
(41) Cotton, F. A.; Frenz, B. A.; Stults, B. R.; Webb, T. R. *J. Am Chem. Soc.* **1976**, *98*, 2768.
(42) Cotton, F. A.; Frenz, B. A.; Ebner, J. R.; Walton, R. A. *Inorg. Chem.* **1976**, *15*, 1861.
(43) Collins, D. A.; Cotton, F. A.; Murillo, C. A. *Inorg. Chem.* **1976**, *15*, 1861.
(44) Cotton, F. A.; Pipal, J. R. *J. Am. Chem. Soc.* **1971**, *92*, 5441.
(45) (a) Cotton, F. A.; Norman, J. G., Jr. *J. Coord. Chem.* **1971**, *1*, 161. (b) Cotton, F. A.; Norman, J. G., Jr. *J. Am. Chem. Soc.* **1972**, *94*, 5697.
(46) Baral, S.; Cotton, F. A.; Ilsley, W. H.; Kaim, W. *Inorg. Chem.* **1982**, *21*, 1644.
(47) van der Helm, D.; Lessor, A E., Jr.; Merritt, L. L., Jr. *Acta Crystallogr.* **1962**, *15*, 1227.
(48) Pauling, L. "The Nature of the Chemical Bond", 3rd ed.; Cornell University Press: Ithaca, NY, 1960; p 224.

of the bridging ligands of the C_{2v} isomer (1.829 Å).

We have obtained indirect evidence for the existence of the D_{4h} isomer in the solid state not complexed by THF.[49]

^{31}P NMR Spectroscopy. A typical ^{31}P NMR spectrum of $Mo_2(S_2PEt_2)_4$ in THF or toluene contains three peaks upfield from $P(OCH_3)_3$, two ~−20 ppm and the third ~−52 ppm. The integrals of these peaks vary with solvent, but the high-field peak and the higher of the two low-field peaks remain essentially equal in area. We surmise from this behavior that two isomers are present, one having a single phosphorus environment (the lowest field resonance) and the second having two phosphorus environments (the two remaining resonances). Since the two crystal structures reported above fit this situation, we assume that the solid-state structures are preserved in solution.

The effect of the diamagnetic anisotropy of the quadruple bond on chemical shifts is such that a nucleus at a position near the horizontal plane intersecting the center of the primary axis (i.e. the M–M vector) will experience substantial deshielding (as in a bridging ligand), while a nucleus lying more nearly along the primary axis will experience a shielding effect (as in a chelating ligand).[26,50] Thus we assign the furthest upfield resonance to the chelating groups of the C_{2v} isomer, the next lower field peak to the bridging groups of the C_{2v} isomer, and the remaining, lowest field peak to the ligands of the D_{4h} isomer. The ^{31}P NMR spectrum of $Mo_2(SOPEt_2)_4$ has resonances only at low field (in particular at ~13 ppm upfield from $P(OCH_3)_3$), and thus the compound appears to contain only bridging Et_2POS groups in toluene solution in agreement with the structure in the crystalline state.[34]

Addition of ~5 equiv of water or THF to a toluene solution of $Mo_2(S_2PEt_2)_4$ produced a negligible effect on the spectrum. The resonances observed for $Mo_2(S_2PEt_2)_4$ in toluene are shifted downfield in THF by ~0.8 ppm for the C_{2v} isomer, while those of the D_{4h} isomer are shifted upfield by ~1.0 ppm. The latter effect is probably a display of the average position of the chemical shifts of THF-complexed and THF-free D_{4h} isomers. Note also that in acetonitrile all three peaks are uniformly shifted downfield by ~4 ppm, by a standard solvent effect.

The peak area of the D_{4h} isomer varied widely but was dependent only on the solvent and not in any way on the source of $Mo_2(S_2PEt_2)_4$. We infer that these two species are in equilibrium and interconvert only slowly on the NMR time scale. We know of no precedent for this type of process for Mo_2L_4 species. Webb et al. have observed facile axial Lewis base coordination with $Mo_2(S_2COR)_4$ species as well as the addition of a fifth S_2COR ligand to such complexes to form $Mo_2(S_2COR)_5^-$ species. Their data suggest that most Lewis base adducts are very labile but that the pentaxanthate species are not.[51]

The equilibrium constant K_{eq} is calculated as the quotient of the integral of the peak due to the D_{4h} isomer divided by the sum of the integrals of the two peaks due to the C_{2v} isomer (i.e., $K_{eq} = [D_{4h}]/[C_{2v}]$).[52] The equilibrium constants calculated presented no significant variation with temperature down to 220 K, and the following data are taken from ambient-temperature spectra.[53] In toluene, $K_{eq} = 0.41$ (1), whereas in THF solution, the equilibrium shifted to a point of about equal concentration of the two isomers ($K_{eq} = 1.21$ (5)). The THF/toluene (50:50) solution had an average K_{eq} of 0.91 (1). The THF complex in toluene had $K_{eq} = 0.45$, while the pyrazine complex in toluene had $K_{eq} = 0.51$. In chloroform solution K_{eq} is 0.44. In acetonitrile solution K_{eq} drops to 0.20 (1). The compound decomposed in pyridine within 2–3 h.

The equilibrium is clearly affected by the solvent. In toluene, a solvent of very low donor number,[54] less than 30% of dissolved $Mo_2(S_2PEt_2)_4$, is present as the D_{4h} isomer. This factor is probably responsible for the observed tendency of the C_{2v} isomer to crystallize out of toluene/hexane solutions. In THF, a solvent of moderate polarity and high donor number, the equilibrium shifts to about 4:5 C_{2v}:D_{4h}. This is probably caused by weak complexation by a THF molecule at an axial Mo coordination site, as seen in the crystal structure of $Mo_2(S_2PEt_2)_4{\cdot}THF$ and in the many other THF adducts of Mo(II) dimers.[3]

The remaining evidence strongly suggests that complexation is the major influence. Both the THF and pyrazine complexes in toluene have slightly increased concentrations of the D_{4h} isomer compared to those of free $Mo_2(S_2PEt_2)_4$. This is particularly significant for the pyrazine complex. Although there have not been other reports of axial pyrazine adducts of Mo(II) dimers, pyridine,[45b,54] THF,[46] and pyrazolylborate[43] adducts have been prepared and characterized. Here, axial coordination of pyrazine is indicated by the single-crystal X-ray structure of the THF adduct and by inference from the marked similarities between the X-ray powder patterns of $Mo_2(S_2PEt_2)_4{\cdot}THF$ and $Mo_2(S_2PEt_2)_4{\cdot}C_4H_4N_2$.

Apparently, acetonitrile does not form an adduct with $Mo_2(S_2PEt_2)_4$. In fact the decrease in K_{eq} going from toluene (dipole moment 0.36 D)[55] to acetonitrile (dipole moment 3.92 D)[56] suggests that Lewis basicity influences not only the equilibrium but also solvent polarity. Here, the influence is as would be predicted from the molecular symmetries; i.e., the C_{2v} isomer (anticipated to have the greater dipole moment) is more favored in the polar medium. The existence of Lewis base adducts of $Mo_2(S_2COR)_4$ complexes with acetonitrile and benzonitrile has been proposed, but apparently these ligands are very loosely bound and easily lost at reduced pressure.[50] Acetonitrile and benzonitrile complexes of tetrahalodimolybdenum(II) have been prepared, but the nitrile ligands apparenty occupy only equatorial sites on the Mo atoms.[57]

The conclusion that we draw from the chemical shift behavior is that the equilibration between the D_{4h} and C_{2v} isomer occurs slowly on the NMR time scale as evidenced by the distinct isomer resonances, though quickly on the laboratory time scale. In contrast, the coordination of axial ligand occurs rapidly on the NMR time scale as evidenced by the chemical shift behavior and the absence of a second D_{4h} isomer resonance (for axial adduct). These are the first clear examples of these kinds of dynamic processes of which we are aware.

Electronic and Vibrational Spectroscopy. Air exposure of

---

(49) The unit cell occupation and symmetry of the second crystal habit found for $Mo_2(S_2PEt_2)_4$ ($Z = 1$ in $P\bar{1}$) requires that the molecule possess C_i point group symmetry. This would be consistent with only tetrabridged (D_{4h}) or tetrachelated (D_{2h} but not D_{2d}) Mo(II) dimers. In light of the ^{31}P NMR results we suspect the former. Difficulties in developing a reliable procedure for the preferential isolation of this habit have precluded further investigation.

(50) San Filippo, J., Jr. *Inorg. Chem.* **1972**, *11*, 3140.

(51) Angell, C. L.; Cotton, F. A.; Frenz, B. A.; Webb, T. R. *J. Chem. Soc., Chem. Commun.* **1973**, 399.

(52) Validity in the determination of the integrals was enhanced by rephasing the spectrum and integrating successively. The results of the integration test with triphenylphosphine and di-*tert*-butylphosphinic acid suggest that ^{31}P NMR integration is a problem in these experiments, and the prescribed gated decoupling experiment merely improves the situation but does not entirely remedy it.

(53) As noted in the Experimental Section, an extensive study of the thermal dependence of the equilibrium was carried out. While random variations in the equilibrium constants were observed, no statistically significant trend in the K_{eq}'s was apparent.

(54) Gutman, V. "The Donor-Acceptor Approach to Molecular Interactions"; Plenum Press: New York, 1978; p 29.

(55) (a) Reference 8, pp 241–243 and references therein. (b) Reference 2 and references therein.

(56) Nelson, R. D., Jr.; Lide, D. R., Jr.; Maryott, A. A. *Natl. Stand. Ref. Data Ser.* (*U.S., Natl. Bur. Stand.*) **1967**, *NSRDS-NBS 10.*

(57) San Filippo, J., Jr.; Sniadoch, H. J.; Grayson, R. L. *Inorg. Chem.* **1974**, *13*, 2121.

the molybdenum bis(phosphinodithioate) derivatives resulted in a color change of the solids from green to dark gray, yet no major changes were observed in the IR spectra of the air-exposed materials except a decrease in the intensity of ν_{sym}(PS) at 490 cm^{-1}. There was no evidence for the formation of Mo=O or Mo—O—Mo bonds as a result of exposure to air since no new bands were observed in the 800–1100-cm^{-1} region.[40,41]

The UV–visible absorption spectrum of $Mo_2(S_2PEt_2)_4$ in toluene has only two bands, at 635 and 335 nm. In THF, these bands are slightly farther apart, bear different intensity ratios at 636 and 334 nm, and are joined by a new absorption at 295 nm. Clark and Franks have reported the electronic spectra of several $Mo_2Cl_8^{4-}$ salts, which have absorptions in the 313–357-nm region and also at 526 nm.[58] Absorptions for tetrahalodimolybdenum(II) complexes have been observed throughout the range 474–666 nm.[57] Trogler and Gray have discussed the electronic spectra and photochemistry of complexes containing quadruple metal–metal bonds and have pointed out the difficulties encountered in assigning the absorption bands in the absence of polarized spectra.[59]

The Raman spectra possess one common band at 346 cm^{-1}. The THF solution and the pyrazine complex in toluene display an additional band at 363 cm^{-1}. Other Mo(II) dimers display Raman bands attributed primarily to M–M stretching vibrations mixed with some M–L stretching vibrations in the range 330–410 cm^{-1}.[3,51,58] The additional new bands seen in the UV–visible and Raman spectra are assigned to an adduct. In $Mo_2(O_2CCF_3)_4$, such a band is found at 397 cm^{-1},[45a] while the band for its bis(pyridine) adduct, $Mo_2(O_2CCF_3)_4 \cdot 2py$, moves down in energy to 367 cm^{-1}.[45b] It appears that a different process occurs in $Mo_2(S_2PEt_2)_4$; i.e., the M–M bond strength increases upon conversion from the C_{2v} structure to the D_{4h} structure, in keeping with the observed Mo–Mo bond shortening.

Magnetic Susceptibilities. All of the phosphinates prepared in this study are weakly paramagnetic with magnetic moments in the range of 0.8–2.0 μ_B/molybdenum atom. The observed moments fall within the range of 0–2.9 μ_B observed for octahedral molybdenum(II) dihalide complexes.[60] The temperature dependence of the susceptibility (Figure 3) did not follow a Curie–Weiss behavior and is not well understood.

Summary and Conclusions

In the family of ligands $R_2PX_2^-$ ($X_2 = S_2$, SO, and O_2) the stereochemistry about molybdenum(II) can be related to the bond angle about X. The sulfur ligand is able to accommodate much smaller angles (typically 85–100°) than oxygen, and we observed the unprecedented mixed, i.e. bridging and chelating, stereochemistry in the C_{2v} isomer of $Mo_2(S_2PEt_2)_4$ as well as the facile interconversion of this form with the all-bridged D_{4h} isomer in solution. The novel equilibrium between these isomers is influenced by the interaction of the D_{4h} isomer with certain bases and by solvent polarity. It is intriguing that the D_{4h} and C_{2v} species are distinguishable in solution (i.e. slow on the NMR time scale) while the coordination of the axial ligand is much faster. With one oxygen and one sulfur in the complex $Mo_2(SOPEt_2)_4$, the larger MoOP angle (typically 120°) precludes chelation and only bridging stereochemistry results. When two such angles are required to be part of a Mo–OPO–Mo system, as in $[Mo(O_2PR_2)_2]_x$, the quadruple bond is split and a weakly paramagnetic polymer results.

Acknowledgment. Financial support of this work by the Cornell University Materials Science Center is gratefully acknowledged. The Cornell University Chemistry Department NMR Facility's Bruker WM300 has been made available by Award CHE7904825 from the National Science Foundation. We also thank Robert P. Micciche for technical assistance, Larry Roe for taking the Raman spectra of $Mo_2(S_2PEt_2)_4$ and its adducts, Prof. J. Campbell Scott and John D. Kulik for making the magnetic measurements, and Prof. Douglas Fitchen and Larry Lichtman for taking the Raman spectrum of $[Mo(O_2PPh_2)_2]_x$.

Registry No. $Mo_2(S_2PEt_2)_4$, 84835-93-8; $Mo_2(S_2PEt_2)_4 \cdot THF$, 84848-83-9; $Mo_2(S_2PEt_2)_4 \cdot C_4H_4N_2$, 84835-94-9; $Mo_2(S_2PPh_2)_4$, 84835-95-0; $Mo_2(SOPEt_2)_4 \cdot THF$, 84835-96-1; $[Mo(O_2PPh_2)_2]_x$, 5163-42-8; $[Mo(O_2PPhMe)_2]_x$, 84835-97-2; $[Mo(O_2POct_2)_2]_x$, 84835-98-3; $K_4Mo_2Cl_8$, 25448-39-9; $(NH_4)_5Mo_2Cl_9$, 61583-95-7; $Mo_2(O_2CCH_3)_4$, 14221-06-8; KS_2PPh_2, 54300-29-7; $KSOPEt_2$, 84835-99-4; $K^+O_2PPh_2^-$, 17223-05-1; $K^+MePhPO_2^-$, 73276-99-0; $K^+Oct_2PO_2^-$, 67206-60-4; Mo, 7439-98-7.

Supplementary Material Available: Figure 3, showing a plot of magnetic susceptibility vs. temperature for $[Mo(n\text{-}Oct_2PO_2)_2]_x$, and listings of observed and calculated structure factors and positional and thermal parameters for $Mo_2(S_2PEt_2)_4$ and $Mo_2(S_2PEt_2)_4 \cdot THF$ (75 pages). Ordering information is given on any current masthead page.

---

[58] Clark, R. J. H.; Franks, M. L. *J. Am. Chem. Soc.* **1975**, *97*, 2691.

[59] Trogler, W. C.; Gray, H. B. *Acc. Chem. Res.*, **1978**, *11*, 232.

[60] (a) Lewis, J.; Nyholm, R. S.; Smith, P. W. *J. Chem. Soc.* **1962**, 2592 and references therein. (b) Colton, R.; Rix, C. J. *Aust. J. Chem.* **1968**, *21*, 1155. (c) Lewis, J.; Nyholm, R. S.; Pande, C. S.; Stiddard, M. H. B. *J. Chem. Soc.* **1963**, 3600. (d) Colton, R.; Tomkins, I. B. *Aust. J. Chem.* **1966**, *19*, 1143, 1519. (e) Drew, M. G. B.; Tomkins, I. B.; Colton, R. *Ibid.* **1970**, *23*, 2517.